Speed control of wound rotor induction motors using chopper controlled external resistance enhanced with a dc capacitor

M.Y. Abdelfattah

Electrical Eng. Dept., Faculty of Engineering, Alexandria University, Alexandria, Egypt

The speed of a wound rotor induction motor can be controlled using chopper controlled external resistance. However, this results in poor efficiency especially at low speeds where the external resistance must be increased extensively. In this paper a new approach is adopted where the speed can be varied continuously using chopper controlled external resistance enhanced with a dc capacitor. With the presence of the additional capacitor the speed can be varied from zero up to the rated value without sacrificing the efficiency of the drive system. The switching operation of the Pulse-Width Modulation (PWM) circuit alters the equivalent resistance in the rotor circuit. It also varies the effective value of the capacitor, which can be considered as a voltage source placed in the rotor circuit. Theoretical analysis is carried out for the drive system. Theoretically obtained results are compared with those obtained experimentally.

من المعروف أنه يمكن التحكم في سرعة الدوران للمحركات الحثية ذات العضو الدوار الملفوف باستخدام مقاومة خارجية مـتحكم فيها بساطور. لكن هذه الطريقة تعطي كفاءة تشغيل منخفضة خاصة عند السرعات المنخفضة حيث تـصبح المقاومـة الخارجيـة المضافة كبيرة للغاية . في هذا البحث تم اقتراح طريقة جديدة للتحكم في سرعة دوران هذه المحركات حيث يمكن تغيير الـسرعة بصورة متصلة باستخدام مقاومة خارجية مدعومة بمكثف متحكم فيهما بساطور. باستخدام المكثف المضاف يمكن تغيـر الـسرعة من الصفر الى القيمة المقننة بدون التضحية بكفاءة التشغيل . يمكن التحكم في سرعة الدوران بنعومة بالتحكم في نـسبة فتـرة الاتصال الى فترة الاستبعاد للمقاومة والمكثف المتصلان معا على التوالي بدائرة العضو الدوار الملفوف من خلال قنطرة تقويم. وتؤدي هذه الطريقة الى تغير القيمة الفعالة للمقاومة المضافة كما تغير القيمة الفعالة للمكثف الذي يعمل كمصدر جهد مضاد لجهد الخرج لقنطرة التقويم المستخدمة . تم اختبار النظام المقترح وتحليله واستعراض النتائج المعملية والنظرية حيث أعطـت تطابقـا ممتازا .

Keywords: Induction motor, Speed control, Rotor circuit control

1. Introduction

Induction motors are the workhorses of industry because of their low cost and rugged construction. They are used in the process-control industry to adjust speed for fans, compressors, pumps, and adjustable-speed induction motor drives used for electric traction. When operated directly from line voltages, induction motors operate at a nearly constant speed. However, by means of power electronic topologies, it is possible to vary their speed efficiently [1].

It is possible to adjust the induction motor speed by controlling only the magnitude of the line voltages applied to the motor [2]. Although simple and inexpensive to implement, this method is extremely energy inefficient if the speed is to be varied over a wide range.

There are various other methods as well, which apply to wound rotor induction motors.

Variable speed operation can be achieved by recovering the slip power [3-4]. This method of speed control is useful in large power applications where variation of speed over a wide range involves a large amount of slip power. Also, controlling the speed of the wound rotor motor can be obtained by resonating the rotor circuit using reactive rotor networks [5]. The problem associated with this technique is the need for exceptionally large capacitance to resonate the rotor circuit.

Another technique, which is similar to that mentioned in ref. [5] is suggested in ref. [6], where switched capacitors in the rotor circuit are used. The speed is varied by varying the duty cycle of four fast acting switches (IGBT) and sixteen fast recovery diodes. Furthermore, the technique requires three capacitors suitable for continuous ac operation.

The simplest method used for controlling the speed of wound rotor induction motors is to convert a fraction of the energy transferred to the rotor circuit into heat through external resistance [7-9]. This method can provide high starting torque. However, using this method, the system becomes inefficient especially at low speeds, where large external resistance is to be added to the rotor circuit. To solve this problem, the present paper proposes a new approach to this technique. An additional dc capacitor is added to the rotor circuit as shown in fig. 1. to enhance the controllability of the drive system as presented in the next section of the paper.

2. System description and simulation

Fig. 2. shows a modified circuit for the chopper controlled wound rotor induction motor. The circuit is referred to the rotor side. The parameters indicated, and the simulation technique used, for the modified model shown in fig. 2, are given in full detail in reference [8]. However, for completion, a quick review for the simulation technique used will be given.
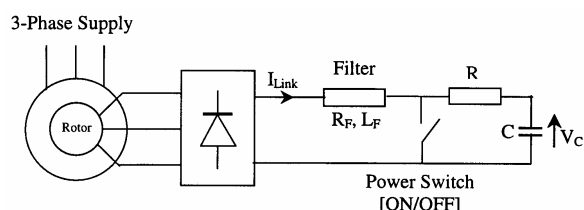

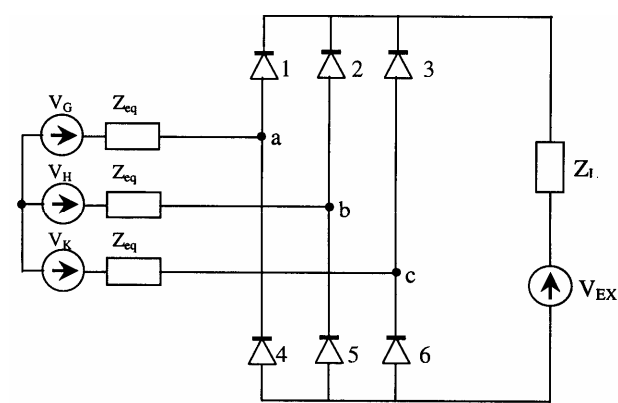Fig. 1. Chopper controlled induction motor enhanced with capacitor.

Fig. 2. Modified circuit for chopper controlled induction motor.

Using stationary reference frame, the three voltages V_G , V_H and V_K and equivalent impedance Z_{eq} shown in fig. 2 are given in per-unit quantities by:

$$V_G = [\omega_r(L_{eq}-L_r)i_{dr} - \omega_r M i_{ds} - (MR_s/L_s)i_{qs} + (M/L_s)V_{qs}] \cos\theta - [\omega_r(L_r-L_{eq})i_{qr} + \omega_r M i_{qs} - (MR_s/L_s)i_{ds} + (M/L_s)V_{ds}] \sin\theta , \qquad (1)$$

$$V_H = [\omega_r(L_{eq}-L_r)i_{dr} - \omega_r M i_{ds} - (MR_s/L_s)i_{qs} + (M/L_s)V_{qs}] \cos(\theta+120^o) - [\omega_r(L_r-L_{eq})i_{qr} + \omega_r M i_{qs} - (MR_s/L_s)i_{ds} + (M/L_s)V_{ds}] \sin(\theta + 120^o), \qquad (2)$$

$$V_K = [\omega_r(L_{eq}-L_r)i_{dr} - \omega_r M i_{ds} - (MR_s/L_s)i_{qs} + (M/L_s)V_{qs}] \cos(\theta-120^o) - [\omega_r(L_r-L_{eq})i_{qr} + \omega_r M i_{qs} - (MR_s/L_s)i_{ds} + (M/L_s)V_{ds}] \sin(\theta -120^o) , \qquad (3)$$

$$Z_{eq} = R_r + pL_{eq} , \qquad (4)$$

$$L_{eq} = (L_rL_s - M^2)/L_s. \qquad (5)$$

The rotor phase voltages V_a, V_b and V_c are given by:

$$V_a = V_G + (R_r+pL_{eq})i_a , \qquad (6)$$

$$V_b = V_H + (R_r+pL_{eq})i_b, \qquad (7)$$

$$V_c = V_K + (R_r+pL_{eq})i_c. \qquad (8)$$

The (d,q) stator voltages V_{qs} and V_{ds} can be defined as;

$$\begin{bmatrix} V_{qs} \\ V_{ds} \end{bmatrix} = \begin{bmatrix} 1 & 0 & 0 \\ 0 & -1/\sqrt{3} & 1/\sqrt{3} \end{bmatrix} \begin{bmatrix} V_A \\ V_B \\ V_C \end{bmatrix} . \qquad (9)$$

The (d,q) rotor voltages V_{qr} and V_{dr} can be defined as:

$$\begin{bmatrix} V_{qr} \\ V_{dr} \end{bmatrix} = \begin{bmatrix} \cos\theta & -\dfrac{1}{\sqrt{3}}\sin\theta & \dfrac{1}{\sqrt{3}}\sin\theta \\ -\sin\theta & -\dfrac{1}{\sqrt{3}}\cos\theta & \dfrac{1}{\sqrt{3}}\cos\theta \end{bmatrix} \begin{bmatrix} V_a \\ V_b \\ V_c \end{bmatrix} . (10)$$

The rotor phase currents i_a , i_b and i_c are given by;

$$\begin{bmatrix} i_a \\ i_b \\ i_c \end{bmatrix} = \begin{bmatrix} \cos\theta & -\sin\theta \\ \cos(\theta+120^o) & -\sin(\theta+120^o) \\ \cos(\theta-120^o) & -\sin(\theta-120^o) \end{bmatrix} \begin{bmatrix} i_{qr} \\ i_{dr} \end{bmatrix}. \quad (11)$$

The above transformations do not give invariance of power, but this is not important in this case since variables are ultimately expressed in the three-phase reference frame.

The differential equations describing the system are given as:

$$pi_{qs} = [L_r V_{qs} - MV_{qr} - \omega_r M^2 i_{ds} - \omega_r ML_r i_{dr}$$
$$-L_r R_s i_{qs} + MR_r i_{qr}]/(L_r L_s - M^2), \quad (12)$$

$$pi_{ds} = [L_r V_{ds} - MV_{dr} + \omega_r M^2 i_{qs} + \omega_r ML_r i_{qr}$$
$$-L_r R_s i_{ds} + MR_r i_{dr}]/(L_r L_s - M^2), \quad (13)$$

$$pi_{qr} = [-MV_{qs} + L_s V_{qr} + \omega_r L_s M i_{ds} + \omega_r L_s L_r i_{dr}$$
$$+MR_s i_{qs} - L_s R_r i_{qr}]/(L_r L_s - M^2), \quad (14)$$

$$pi_{dr} = [-MV_{ds} + L_s V_{dr} + \omega_r L_s M i_{qs} - \omega_r L_s L_r i_{qr}$$
$$+MR_s i_{ds} - L_s R_r i_{dr}]/(L_r L_s - M^2), \quad (15)$$

$$p\omega_r = [T_E - T_L - T_D]/J, \quad (16)$$

$$p\theta = \omega_r , \quad (17)$$

where in per-unit quantities the electromagnetic torque T_E is given by:

$$T_E = M[i_{dr}i_{qs} - i_{qr}i_{ds}]. \quad (18)$$

Here, the chopper electronically alters the effect of the R-C series combination in a continuous and contact-less manner. The duty cycle of the chopper is controlled by a PWM firing circuit. With the presence of the additional capacitor with the resistor the speed can be varied from zero up to the full rated value.

During ON/OFF operation of the power switch the equivalent impedance Z_L seen by the rectifier bridge varies from $[R_F + pL_F]$ to $[(R_F + R) + pL_F]$, respectively. Also, V_{EX} varies from 0 to $+V_C$, respectively. Choosing branches (diodes) 1,2,3,4 and 5 as links, we obtain five basic loops. Each basic loop contains only one link. When the power switch is ON an

additional loop exists which is the R-C series combination shorted by the power switch. The equation governing the shorted circuit is, therefore,

$$C(dV_C/dt) = - V_C/R. \quad (19)$$

When the switch is OFF the equation governing the capacitor voltage is,

$$C(dV_C/dt) = I_{Link} . \quad (20)$$

The basic loops voltage array described in ref. [8] is now redefined as:

$$\mathbf{E}_{loop} = \begin{bmatrix} V_G - V_K - V_{EX} \\ V_H - V_K - V_{EX} \\ -V_{EX} \\ V_G - V_K \\ V_H - V_K \end{bmatrix} . \quad (21)$$

The performance equation of the network in the loop reference frame can be written in the form:

$$\mathbf{E}_{loop} = \mathbf{Z}_{loop} \, \mathbf{I}_{loop} , \quad (22)$$

where $\mathbf{Z}_{loop}$ is given by:

$$\mathbf{Z}_{loop} = \begin{bmatrix} Z_L + 2Z_{eq} & Z_L + Z_{eq} & Z_L & 2Z_{eq} & Z_{eq} \\ Z_L + Z_{eq} & Z_L + 2Z_{eq} & Z_L & Z_{eq} & 2Z_{eq} \\ Z_L & Z_L & Z_L & 0 & 0 \\ 2Z_{eq} & Z_{eq} & 0 & 2Z_{eq} & Z_{eq} \\ Z_{eq} & 2Z_{eq} & 0 & Z_{eq} & 2Z_{eq} \end{bmatrix} .$$

$$(23)$$

Eq. (22) represents five independent equations if all six diodes are conducting. However, when only two diodes are conducting, these equations are reduced to only one equation. If only three diodes are conducting these equations are reduced to only two equations, etc.[10]. The situation of rectifier bridge can be defined in an array named rectifier state-array **S** having 1 or 0 depending on whether the diode is conducting or not respectively [10]. The matrix connecting the existing loops with those if all diodes are conducting is $\mathbf{C}_n$. The construction of $\mathbf{C}_n$ is obtained from the previous knowledge of **S** [10]. The

transformation process gives the voltage and current vectors for the new network as:

$$\mathbf{V}_n = \mathbf{C}_n{}^t \, \mathbf{E}_{loop}, \tag{24}$$

$$\mathbf{I}_{loop} = \mathbf{C}_n \, \mathbf{I}_n. \tag{25}$$

The new impedance matrix is given by:

$$\mathbf{Z}_n = \mathbf{C}_n{}^t \, \mathbf{Z}_{loop} \, \mathbf{C}_n \, , \tag{26}$$

from which the following equation can be written:

$$\mathbf{V}_n = \mathbf{Z}_n \, \mathbf{I}_n = [\mathbf{R}_n + p\mathbf{L}_n] \, \mathbf{I}_n, \tag{27}$$

from which we get the new current derivatives at any time t as :

$$p\mathbf{I}_n = \mathbf{L}_n{}^{-1} \, [\, \mathbf{V}_n - \mathbf{R}_n \, \mathbf{I}_n \,]. \tag{28}$$

When all six diodes are conducting, the voltage drop across each of them is zero, and eq. (22) holds good. However, if any diode is open, then a voltage will appear across it. It is necessary to calculate this voltage to check whether a new diode is to be included in the conducting pattern or not. To calculate this voltage, eq. (22) will be modified to the form:

$$\mathbf{V}_x = \mathbf{E}_{loop} - \mathbf{Z}_{loop} \, \mathbf{I}_{loop} \, . \tag{29}$$

From the previous choice of links, we find that diode number 6 is the dependent diode; then V_x is expressed as:

$$\mathbf{V}_x = \begin{bmatrix} V_1 + V_6 \\ V_2 + V_6 \\ V_3 + V_6 \\ -V_4 + V_6 \\ -V_5 + V_6 \end{bmatrix} , \tag{30}$$

where V_j is the voltage across the jth diode.

3. Theoretical and experimental results

The system parameters used are as follows:
1- Induction motor : 380V, Y-connected, 6.5A, 2.2kW, 50Hz, 4-pole, wound rotor. The parameters are :
$R_s = 1.83 \; \Omega \, , \quad R_r = 0.275 \; \Omega, \quad L_s = 243.9$ mH, $L_r = 20.2$ mH

$M = 234$ mH $J = 0.06$ kg-m^2
$N_r \, / \, N_s = 78 \, / \, 271$
2- Filter : $R_F = 1.145 \; \Omega \, , \quad L_F = 57.22$ mH.
3- R-C series combination: $R = 5.65\Omega, C = 240 \; \mu F$.

The system has been tested and evaluated. During the operation, the chopper frequency f_{CH} was adjusted to $f_{CH} = 200$Hz, and the supply line voltage was 280V. This supply line voltage, (280V), was chosen because of the constraint imposed by the forward voltage for the transistor used (V_{ceo} max. = 160V). For simulation purpose a computer program written in Pascal language was prepared.

For current measurements during experimental tests a standard shunt resistance having a value of 0.11Ω was used. Accordingly, when a current is to be calculated the vertical scale for this current has to be multiplied by (1/0.11 = 9.1 Amp/Volt).

The following tests were performed:
Test 1: This shows the steady-state performance for the drive system with chopper duty cycle $\lambda = 0.64$ and a load torque $T_L = 6.5$ N.m. Fig. 3 shows the actual system performance, (experimental results), while fig. 4 shows the predicted performance for the same conditions. The steady-state measured speed is 633 rpm, while the predicted speed is 639 rpm.

Several measurements were taken for the system at steady state. Fig. 5 shows the relationship between the speed of the motor and the load torque for different duty cycles.

Fig. 6 shows the relationships between the speed of the motor and chopper duty cycle for constant load torque. Figs. 5 and 6 indicate the possibility of achieving high starting torque. For example, a starting torque of 9 N.m. can be achieved with duty cycle $\lambda = 0.59$. It should be noted that fig. 5 is extracted from fig. 6.
Test 2: This is a comparison test. The speed range of the proposed approach is compared with the case using additional resistance alone [8]. The drive system was tested for the same load torque $T_L = 6.5$ N.m. As fig. 7 indicates, the speed range is zero rpm to 1239 rpm for duty cycle varying from 0.463 to 1.0 for the proposed approach. The speed range is 320 rpm to 1239 rpm for a duty cycle varying from zero to 1.0 for the case using additional resistance alone. So, the proposed approach

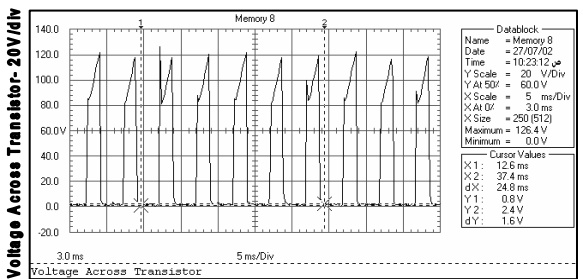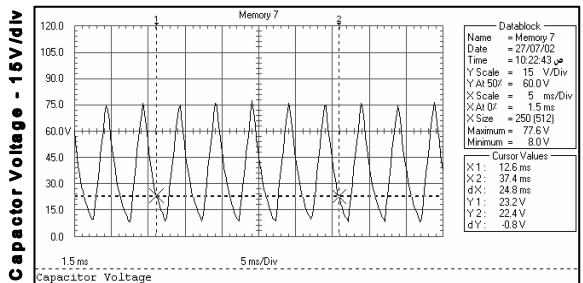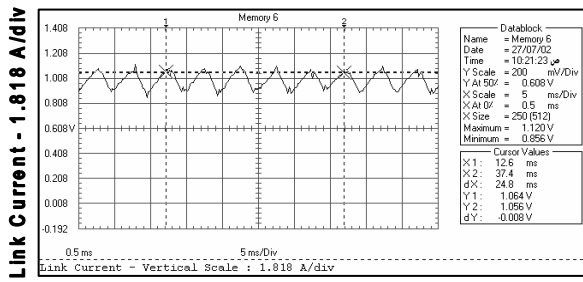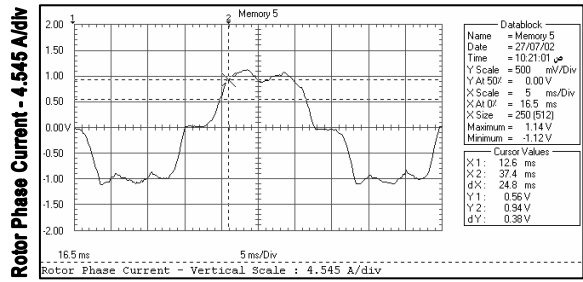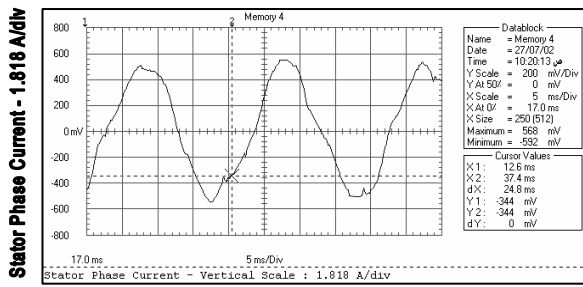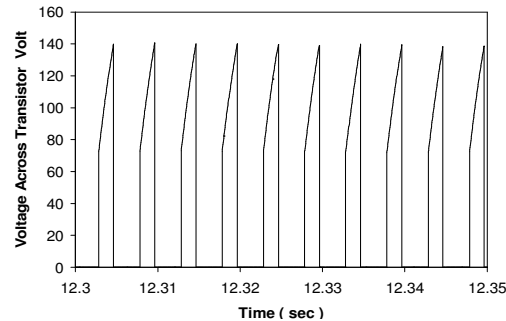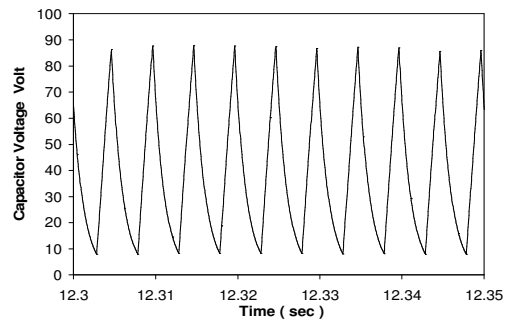provides a wider range of speed variation for
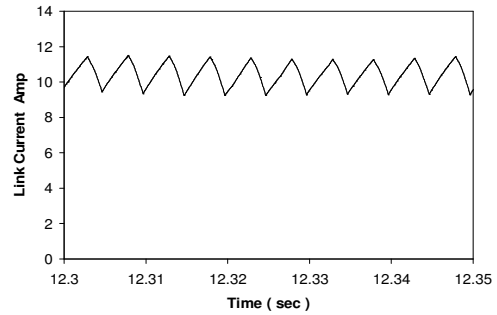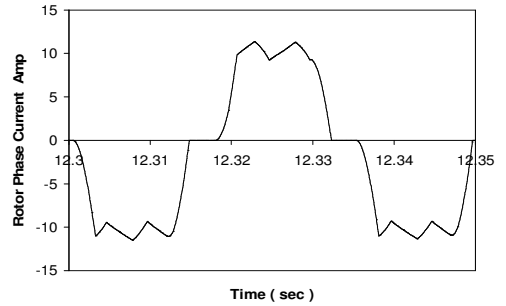
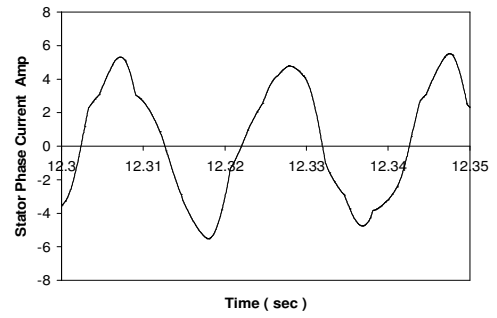Fig. 3. Experimental results for test 1.

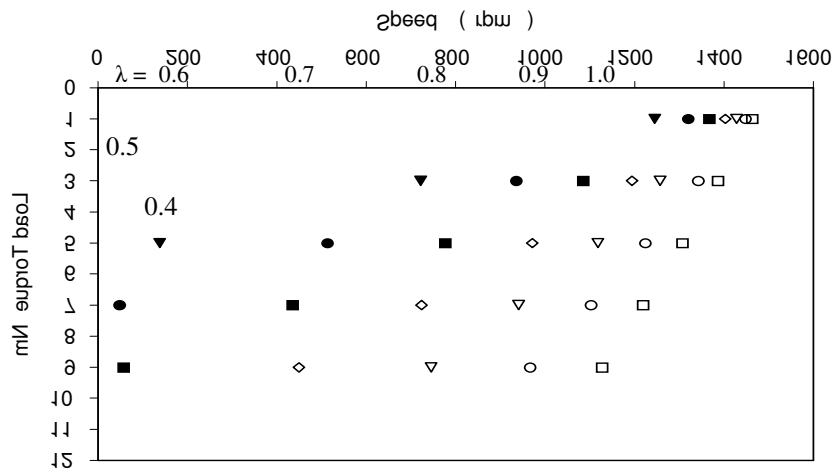Fig. 4. Simulation results for test 1.

Fig. 5. [Load torque / speed] for constant duty cycle.
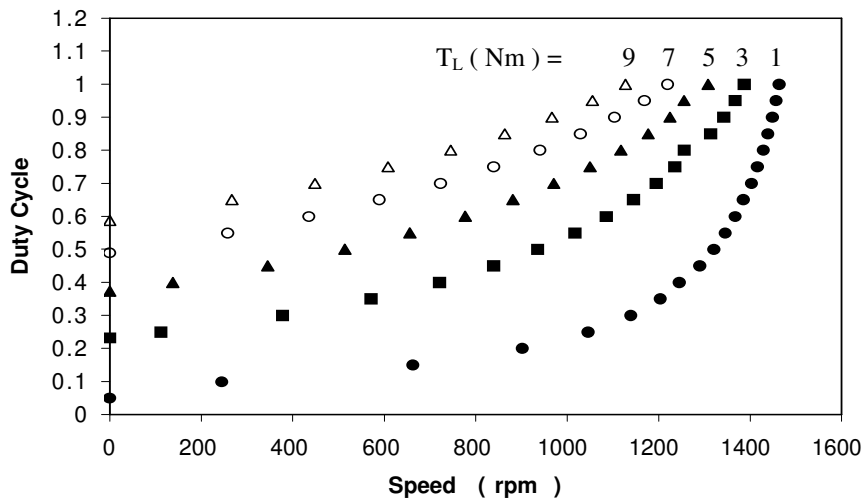

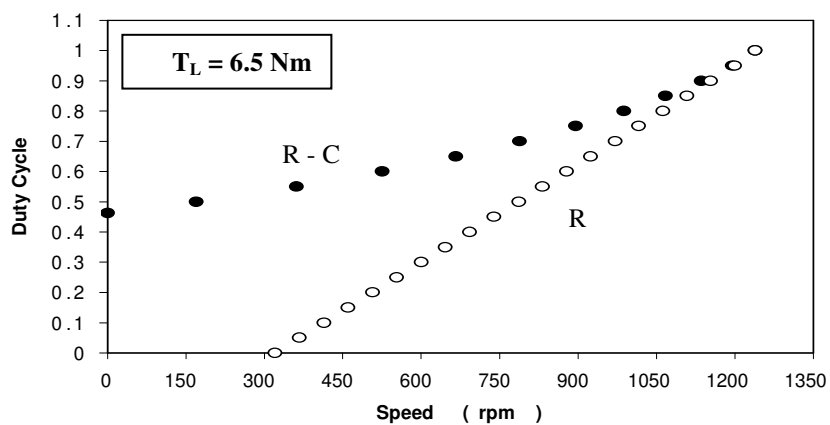Fig. 6. [Duty cycle / speed] for constant load torque.

Fig. 7. [Duty cycle / speed] for test 2.

the same load torque when compared with the case using additional resistance alone.

Test 3: This is a transient test. The duty cycle is adjusted to $\lambda = 0.64$. The load torque applied to the rotor shaft is given by : $T_L =$ 10.32×10^{-3} n_r N.m where n_r is the motor speed in rpm. Fig. 8 shows the actual system performance, (experimental results), while fig. 9 shows the predicted performance for the same test.
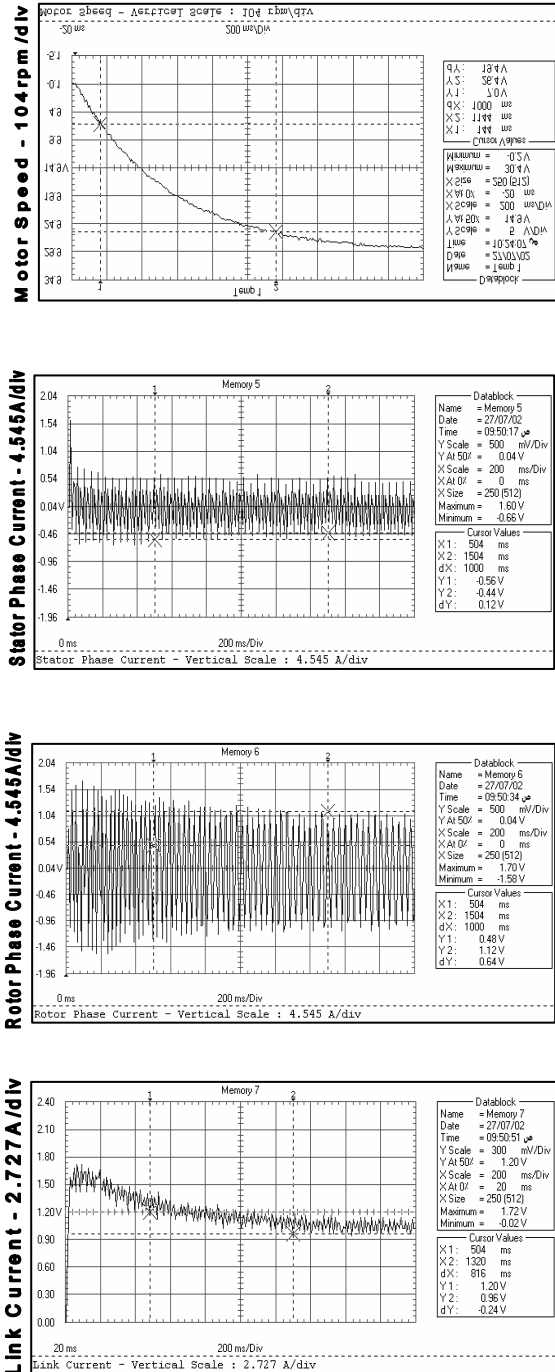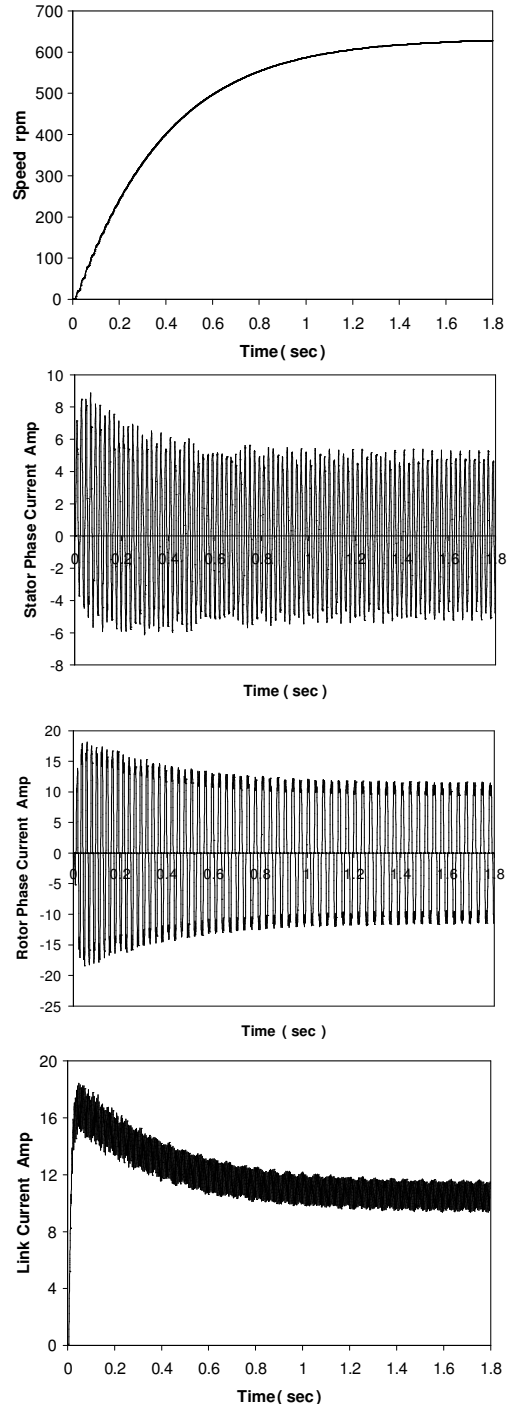

Fig. 8. Experimental results for test 3.

Fig. 9. Simulation results for test 3.

4. Closed loop operation

To investigate the possibility of the new configuration to work on closed loop control strategy, two types of controllers are suggested. These are, proportional controller (*P*), and proportional + integral controller (*PI*). The transfer functions of the suggested controllers are as follows:

$$G_C(s) = K_P \qquad\qquad P-Controller,$$

$$G_C(s) = K_P(1 + \frac{1}{T_i s}) \qquad PI-Controller.$$

Many approaches have been developed to tune these controllers [11]. Ziegler-Nichols open-loop tuning method is used here. The parameters for these two controllers according to this tuning method are as follows:

for P–controller : $K_P = 9.60 \times 10^{-3}$ /rpm,
for PI–controller : $K_P = 8.64 \times 10^{-3}$ /rpm, and
$T_i = 222.8$ msec.

Fig. 10 shows the suggested closed-loop control system.

The closed-loop control system was theoretically investigated for variable speed drive operation, as well as for constant speed
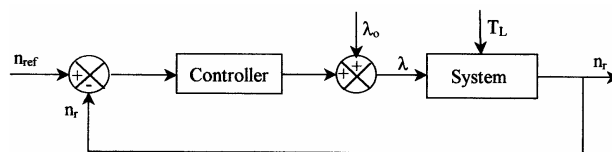

Fig. 10. Controller feedback system.

drive operation. Fig. 11 shows the predicted performance, using the simulation technique described in section 2, for variable speed operation. While the motor is loaded with $T_L = 6$ N.m and the duty cycle $\lambda = 0.5$, the reference speed was changed from 287 rpm to 850.6 rpm.

For the P–controller the speed reached only 830.8 rpm, with a steady-state speed error of –19.8 rpm. This steady-state error is zero for the PI–controller as expected.

Fig. 12 shows the predicted performance for constant speed operation. While the motor is loaded with 9 N.m and duty cycle $\lambda = 0.75$ a speed of 607.1 rpm is observed. A sudden change is made to the load torque so that $T_L = 6$ N.m. For the P–controller the speed changed to 622.3 rpm, with a steady-state speed error of +15.2 rpm. This steady-state error is again zero for the PI–controller.
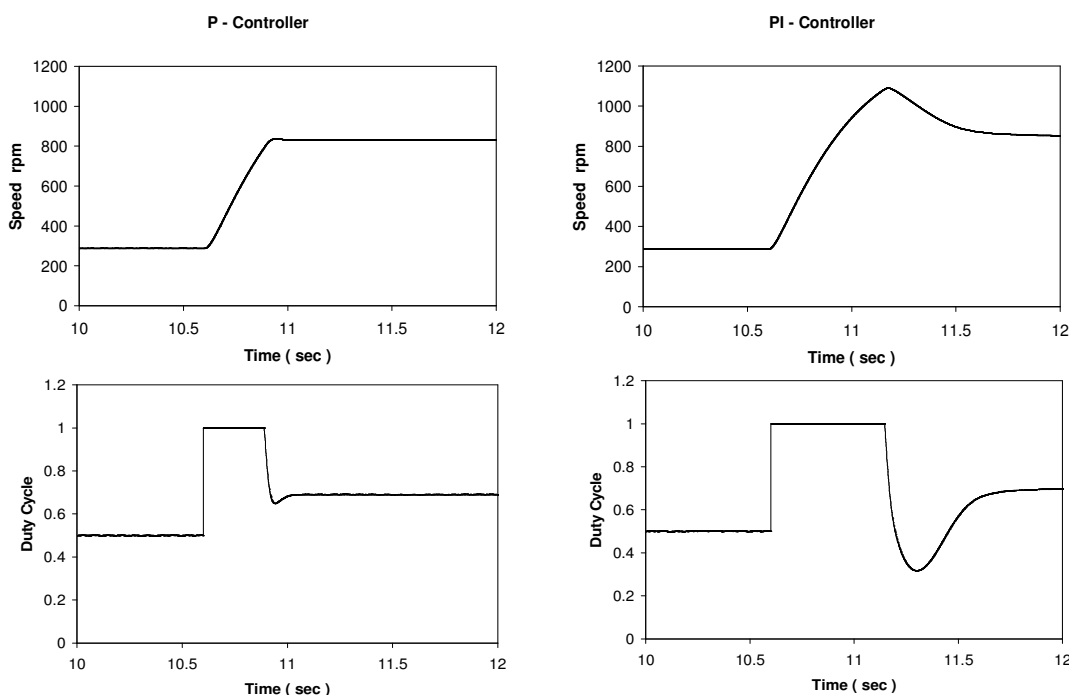

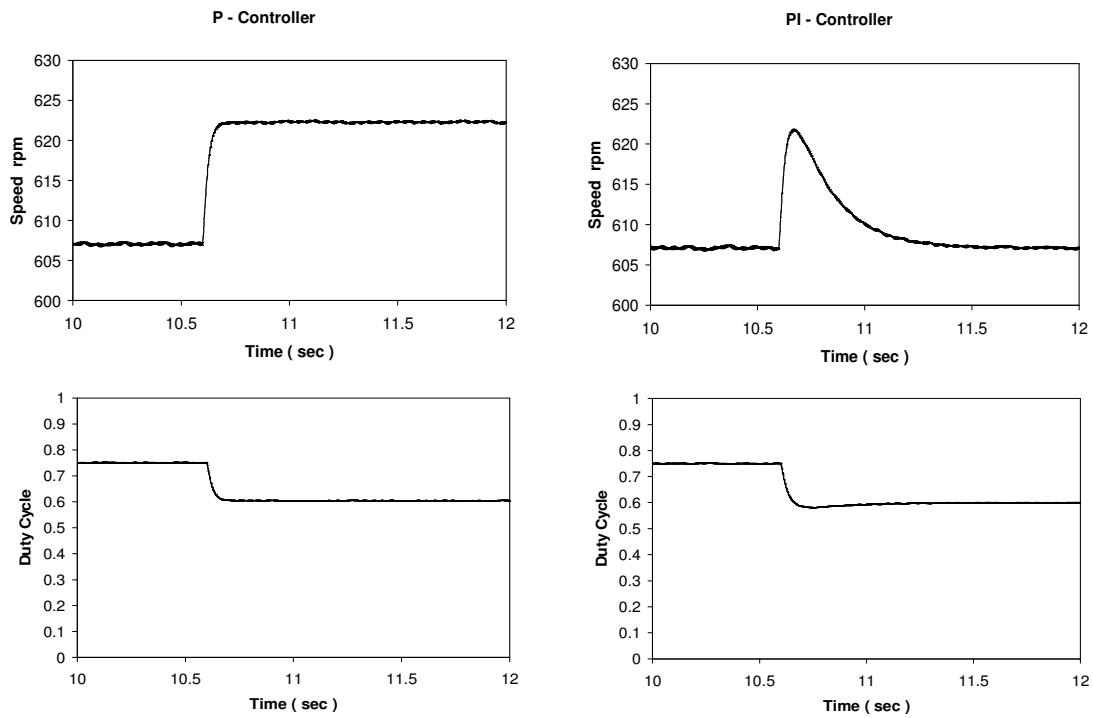Fig. 11. Variable speed operation for p- and pi-controllers.

Fig. 12. Constant speed drive operation for P- and PI-controllers.

5. Conclusions

A new topology for chopper controlled wound rotor induction motor is presented. The new approach is characterized with simplicity, low cost, high efficiency, wide range of speed control, possibility for satisfactory closed loop operation, possibility for high starting torque operation, and above all the requirement of only few number of switching devices. Only six power diodes and one power transistor are used, which contributes very much to the high efficiency operation. Comparison between experimental results and those obtained theoretically shows good correlation between them. The percentage error between measured and simulation results for maximum stator current, maximum rotor current, maximum capacitor voltage, and maximum transistor voltage are 6.3%, 8%, 9.5%, and 10.7% respectively. Figs. 11 and 12 showed that the proposed approach works satisfactorily with closed-loop feedback systems. For zero steady-state error the PI-controller is suggested.

Notations

A,B,C Suffices indicating stator variables as in V_A,

a,b,c Suffices indicating rotor variables as in V_a,

s Suffix indicating stator quantity as in L_s,

r Suffix indicating rotor quantity as in L_r,

q,d Suffices indicating q and d axes, respectively,

i_{qs},i_{ds} q,d axes equivalent stator currents,

i_{qr},i_{dr} q,d axes equivalent rotor currents,

R_s, R_r Stator and rotor Resistance / phase, respectively.

L_s, L_r Apparent three phase stator and rotor inductance / phase, respectively,

M Apparent three phase mutual inductance / phase,

ω_r Rotor angular speed,

θ Angle between stator phase A and rotor phase a ,

J Moment of inertia,

T_L Load torque,

T_D Damping torque,

R Added resistance to rotor side,

R_F, L_F Filter resistance and inductance, respectively,

N_r / N_s Rotor to stator turns ratio,

f_{CH} Chopper frequency ,

T_{ON} Chopper on period,

T_{CH} Chopping period ($T_{CH} = 1/f_{CH}$) , and

λ Chopper duty cycle ($\lambda = T_{ON}/T_{CH}$) .

References

[1] P.C. Sen, "Electric Motor Drives and Control – Past, Present and Future", IEEE Trans. On Industrial Electronics, Vol. 37 (6), pp. 562-575 (1990).

[2] V.V. Sastry, M.R. Prasad, and T.V. Sivakumar, "Optimal soft Starting of Voltage-Controller fed IM Drive Based on Voltage Thyristors", IEEE Trans. On Power Electronics, Vol. 12 (6), pp. 1041-1059 (1997).

[3] S.R. Doradla, S. Chakravorty, and K.E. Hole, "A New Slip Power Recovery Scheme with Improved Supply Power Factor", IEEE Trans. On Power Electronics, Vol. 3 (2), pp. 200-207 (1988).

[4] M.Y. Abdelfattah, A.L. Mohamadein, and T.E. Sharaf, "Performance Study for Slip-Energy Recovery Drive", Fifth International Middle East Power Conference MEPCON'97, Alexandria, Egypt, January 4-6, pp. 156-164 (1997).

[5] J. Reinert and G.M.J. Parsley, "Controlling the Speed of an Induction Motor by Resonating the Rotor Circuit", IEEE Trans. On Industry Applications, Vol. 31 (4), pp. 887-891 (1995).

[6] A.E. Lashine, S.M.R. Tahoun, and F.A. Safaan, "A New Approach to the Speed Control of Wound-Rotor Induction Motors", Alexandria Engineering Journal AEJ, Vol. 38 (3), Section B, pp. B75-B85 (1999).

[7] M. Ramamoorty and M. Arunachalam, "Dynamic Performance of a Closed Loop Induction Motor Speed Control System with Phase-Controlled SCR's in the Rotor", IEEE Trans. On Industry Applications, Vol. 15 (5), pp. 489-493 (1979).

[8] M.Y. Abdelfattah and A.R. Abdelaziz, "Performance study of a Chopper-Controlled Induction Motor", Electric Machines and Power Systems Journal, Vol. 19 (1), pp. 81-102 (1991).

[9] S. Lesan, M.S. Smiai and W. Shephert, "Control of Wound Rotor Induction Motor Using Thyristors in the Secondary circuits", IEEE Trans. On Industrial Applications, Vol. 32 (2), pp. 335-344 (1996).

[10] S. Williams and I.R. Smith, "Fast Digital Computation of 3-Phase Thyristor Bridge Circuits", Proc. IEE, Vol. 120 (7), pp. 791-795 (1973).

[11] W.K.Ho, O.P. Gan, E.B. Tay and E.L. Ang, "Performance and Gain and Phase Margins of Well-Known PID Tuning Formulas", IEEE Trans. On Control System Technology, Vol. 4, pp. 473-477 (1996).